

INTEGRAL discovery of a burst with associated radio emission from the magnetar SGR 1935+2154

S. MEREGHETTI

INAF – Istituto di Astrofisica Spaziale e Fisica Cosmica, Via A. Corti 12, I-20133 Milano, Italy

V. SAVCHENKO, C. FERRIGNO

ISDC, Department of Astronomy, University of Geneva, Chemin d'Écogia, 16 CH-1290 Versoix, Switzerland

D. GÖTZ

AIM-CEA/DRF/Irfu/Département d'Astrophysique, CNRS, Université Paris-Saclay, Université de Paris, Orme des Merisiers, F-91191 Gif-sur-Yvette, France

M. RIGOSELLI

INAF – Istituto di Astrofisica Spaziale e Fisica Cosmica, Via A. Corti 12, I-20133 Milano, Italy

A. TIENGO

Scuola Universitaria Superiore IUSS, Piazza della Vittoria n.15, I-27100 Pavia, Italy

A. BAZZANO

INAF – Institute for Space Astrophysics and Planetology, Via Fosso del Cavaliere 100, I-00133 Rome, Italy

E. BOZZO

ISDC, Department of Astronomy, University of Geneva, Chemin d'Écogia, 16 CH-1290 Versoix, Switzerland

A. COLEIRO

APC, AstroParticule et Cosmologie, Université Paris Diderot, CNRS/IN2P3, CEA/Irfu, Observatoire de Paris Sorbonne Paris Cité, 10 rue Alice Domont et Léonie Duquet, F-75205 Paris Cedex 13, France.

T. J.-L. COURVOISIER

ISDC, Department of Astronomy, University of Geneva, Chemin d'Écogia, 16 CH-1290 Versoix, Switzerland

M. DOYLE

Space Science Group, School of Physics, University College Dublin, Belfield, Dublin 4, Ireland

A. GOLDWURM

APC, AstroParticule et Cosmologie, Université Paris Diderot, CNRS/IN2P3, CEA/Irfu, Observatoire de Paris Sorbonne Paris Cité, 10 rue Alice Domont et Léonie Duquet, F-75205 Paris Cedex 13, France.

L. HANLON

Space Science Group, School of Physics, University College Dublin, Belfield, Dublin 4, Ireland

E. JOURDAIN

*CNRS; IRAP; 9 Av. colonel Roche, BP 44346, F-31028 Toulouse cedex 4, France
Université de Toulouse; UPS-OMP; IRAP; Toulouse, France*

A. VON KIENLIN

Max-Planck-Institut für Extraterrestrische Physik, Garching, Germany

A. LUTOVINOV

*Moscow Institute of Physics and Technology, Institutskiy per. 9, 141700 Dolgoprudny, Moscow Region, 141700, Russia
Space Research Institute of Russian Academy of Sciences, Profsoyuznaya 84/32, 117997 Moscow, Russia*

A. MARTIN-CARRILLO

Space Science Group, School of Physics, University College Dublin, Belfield, Dublin 4, Ireland

S. MOLKOV

*Moscow Institute of Physics and Technology, Institutskiy per. 9, 141700 Dolgoprudny, Moscow Region, 141700, Russia
Space Research Institute of Russian Academy of Sciences, Profsoyuznaya 84/32, 117997 Moscow, Russia*

L. NATALUCCI, F. ONORI, F. PANESSA, J. RODI

INAF – Institute for Space Astrophysics and Planetology, Via Fosso del Cavaliere 100, I-00133 Rome, Italy

J. RODRIGUEZ

*AIM-CEA/DRF/Irfu/Département d'Astrophysique, CNRS, Université Paris-Saclay, Université de Paris,
Orme des Merisiers, F-91191 Gif-sur-Yvette, France*

C. SÁNCHEZ-FERNÁNDEZ

European Space Astronomy Centre (ESA/ESAC), Science Operations Department, 28691 Villanueva de la Caada, Madrid, Spain

R. SUNYAEV

*Space Research Institute of Russian Academy of Sciences, Profsoyuznaya 84/32, 117997 Moscow, Russia
Max Planck Institute for Astrophysics, Karl-Schwarzschild-Str. 1, Garching b. D-85741, Munchen, Germany*

AND P. UBERTINI

INAF – Institute for Space Astrophysics and Planetology, Via Fosso del Cavaliere 100, I-00133 Rome, Italy

(Received ; Revised ; Accepted)

Submitted to ApJ Letters

ABSTRACT

We report on observations of the soft γ -ray repeater SGR 1935+2154 carried out with the INTEGRAL satellite between 2020 April 28 and May 3, during a period of bursting activity. Several short bursts with fluence in the range $\sim 10^{-7} - 10^{-6}$ erg cm $^{-2}$ were detected by the IBIS instrument in the 20-200 keV range. The burst with the hardest spectrum, discovered and localized in real time by the INTEGRAL Burst Alert System, was spatially and temporally coincident with a fast radio burst detected by the CHIME and STARE2 radio telescopes at 400-880 MHz and 1.5 GHz, respectively. The burst light curve in the 20-200 keV range shows two peaks separated by ~ 30 ms, superimposed on a broad pulse lasting ~ 0.4 s. The burst spectrum over 0.3 s is well fit with an exponentially cut-off power law with photon index $\Gamma = 0.75 \pm 0.3$, e-folding energy $E_0 = 52^{+14}_{-8}$ keV, and 20-200 keV flux $(1.5 \pm 0.1) \times 10^{-6}$ erg cm $^{-2}$ s $^{-1}$. This is the first burst with a radio counterpart observed from a soft γ -ray repeater and it strongly supports the models based on magnetars that have been proposed for extragalactic fast radio bursts, despite the energy budget involved in the SGR 1935+2154 burst is a factor $\sim 10^{8-9}$ smaller than that of sources at distances of hundreds of Mpc. We also estimate for SGR 1935+2154 a distance in the range $\sim 2-7$ kpc, based on the analysis of an expanding dust scattering ring seen in X-rays with the *Neil Gehrels Swift Observatory* XRT instrument.

Keywords: Stars: magnetars - Stars: individual (SGR 1935+2154) - Fast radio bursts

1. INTRODUCTION

Magnetars are neutron stars powered mainly by magnetic energy dissipation that are characterized by strong variability on several timescales (see [Mereghetti et al. 2015](#); [Turolla et al. 2015](#); [Kaspi & Beloborodov 2017](#) for reviews). Many magnetars were first discovered as Soft Gamma-Ray Repeaters (SGRs), i.e. sources of multiple bursts of hard X-rays, typically shorter than 1 s and with peak luminosity up to $\sim 10^{39-41}$ erg s $^{-1}$. Longer and more energetic outbursts have also been observed from a few SGRs, with the most extreme cases, known as Giant Flares, reaching peak luminosity as large as 10^{47} erg s $^{-1}$ and releasing a total energy up to 10^{46} erg (e.g., ([Palmer et al. 2005](#))). All the currently known magnetars are in the Galaxy or in the Magellanic Clouds ([Olausen & Kaspi 2014](#)).

Fast Radio Bursts (see ([Cordes & Chatterjee 2019](#); [Petroff et al. 2019](#)) for reviews) are an enigmatic class of sources emitting short ($\sim 1 - 10$ ms) pulses of radio emission with peak fluxes of $\sim 0.1 - 100$ Jy at 1.4 GHz, and dispersion measures (DM) in excess of the Milky Way values along their lines of sight. Their extragalactic nature has been demonstrated by the association of a few FRBs with galaxies at redshifts from $z = 0.0337$ ([Marcote et al. 2020](#)) to $z = 0.66$ ([Ravi et al. 2019](#)). A large variety of models have been proposed for the FRB (see [Platts et al. 2019](#) for an extensive and updated list), but no consensus has been reached yet on the nature of these sources. Although many of these models involve magnetars, there has been no confirmed association between an FRB and a high-energy bursting source until now.

Here we report on observations of the magnetar SGR 1935+2154 carried out with the INTEGRAL satellite in April-May 2020. In particular, we present the properties of a short and hard burst for which a spatially and temporally coincident FRB has been detected in the 400-800 MHz band ([Scholz & Chime/Frb Collaboration 2020](#)) and at 1.4 GHz ([Bochenek et al. 2020](#)). This is the first detection of a pulse of radio emission clearly associated with an SGR burst, thus providing an intriguing connection between magnetars and FRB. We also report a new estimate of the distance of SGR 1935+2154 based on the analysis of a dust scattering ring recently detected with the *Neil Gehrels SWIFT Observatory* ([Kennea et al. 2020](#)).

2. SGR 1935+2154

SGR 1935+2154 was discovered through the detection of hard X-ray bursts with Swift/BAT in July 2014 ([Stamatikos et al. 2014](#)). Its magnetar nature was confirmed

Table 1. Log of observations in April-May 2020 and number of bursts detected with IBIS/ISGRI.

Start time MM-DD HH:MM (UTC)	End time MM-DD HH:MM (UTC)	ON-time ^a ks	Off-axis angle(°)	# of bursts
04-22 18:54	04-23 07:44	41.1(89%)	6.2 – 17.0	0
04-25 10:46	04-26 01:29	42.8(80%)	4.2 – 18.6	0
04-28 02:37	04-29 12:54	102.6(83%)	0.5 – 18.2	8
04-30 18:27	04-30 23:08	8.6(51%)	12.9 – 16.0	0
05-01 02:08	05-01 04:27	7.9(94%)	15.4 – 19.0	0
05-01 11:51	05-01 14:10	7.9(95%)	13.1 – 16.0	0
05-01 17:10	05-01 19:29	7.9(94%)	15.4 – 19.0	0
05-03 10:53	05-05 05:30	127.3(82%)	0.6 – 18.4	1

^aThe source ON-time takes into account the bad time intervals, due to, e.g., telemetry gaps. Between parentheses, the fraction of time with the source in the IBIS/ISGRI field of view.

by follow-up X-ray observations that revealed a spin period $P = 3.25$ s and period derivative $\dot{P} = 1.43 \times 10^{-11}$ s s $^{-1}$ ([Israel et al. 2016](#)), corresponding to a characteristic age of 3.6 kyr and dipole magnetic field of 2.2×10^{14} G. A very faint (H \sim 24) near infrared counterpart was identified, thanks to its variability, by the Hubble Space Telescope ([Levan et al. 2018](#)). Pulsed radio emission has been observed in a few transient magnetars, but not in SGR 1935+2154 ([Burgay et al. 2014](#); [Surnis et al. 2014](#); [Israel et al. 2016](#); [Pearlman et al. 2020](#)), with the most constraining upper limits of $14 \mu\text{Jy}$ (4.6 GHz) and $7 \mu\text{Jy}$ (1.4 GHz) derived by [Younes et al. \(2017\)](#). Single pulses were also undetected down to limits of ~ 70 mJy ([Israel et al. 2016](#)) and ~ 10 -20 mJy ([Younes et al. 2017](#)).

Like most known magnetars, SGR 1935+2154 lies in the Galactic Plane ($l=57.25$, $b=0.82$), at an unknown distance. The magnetar could be associated with the supernova remnant G57.2+0.8, for which distances of ~ 12.5 kpc ([Koches et al. 2018](#)) and 4.5–9 kpc ([Ranasinghe et al. 2018](#)) have been derived. In the following, we will scale all the quantities to an assumed distance of $d = 10d_{10}$ kpc.

Since its discovery, SGR 1935+2154 has been rather active, emitting short bursts in February 2015 and May-July 2016 ([Younes et al. 2017](#); [Lin et al. 2020](#)), as well as an intermediate flare on April 12, 2015 ([Kozlova et al. 2016](#)). Recently, SGR 1935+2154 has entered a new period of activity ([Hurley et al. 2020](#); [Veres et al. 2020](#)) that culminated with the emission of a “burst forest”, i.e. tens of bursts in a short time interval, on April 27-28 ([Palmer 2020](#); [Younes et al. 2020](#); [Fletcher & Fermi GBM Team 2020](#)).

3. INTEGRAL DATA ANALYSIS AND RESULTS

The position of SGR 1935+2154 was repeatedly inside the 30×30 deg² field of view of the IBIS instrument (Ubertini et al. 2003), for a total on-time of ~ 350 ks between 18:54 of April 22 and 05:30 UT of May 5, 2020 (see Table 1 for the exact times and different off-axis angles of the source). The data of the IBIS/ISGRI detector (Lebrun et al. 2003) are analyzed in real time at the INTEGRAL Science Data Center (ISDC, Courvoisier et al. (2003)) by the INTEGRAL Burst Alert System (IBAS), a software for the automatic search and rapid localization of gamma-ray bursts and other transient sources (Mereghetti et al. 2003).

IBAS triggered on two events at 09:51:05 UTC and 14:34:24 UTC of April 28 and automatically distributed the public Alert Packets reporting the identification of SGR 1935+2154 as the origin of these triggers less than 10 s after the bursts. An analysis of the ISGRI data carried out off-line with the standard imaging analysis software (Goldwurm et al. 2003) confirmed the association of both events with SGR 1935+2154.

A more sensitive search for other bursts was carried out off-line by examination of mask-tagged light curves of SGR 1935+2154 on timescales of 10 ms, 100 ms, and 1 s, extracted using the `ii_light` program. This resulted in the discovery of other seven bursts (see Table 2), that were missed by the IBAS software due to their large off-axis angles.

The background-subtracted ISGRI light curve (20-200 keV) of the brightest of the two bursts detected by IBAS (burst-G) is shown in Fig. 1, where the time refers to the geocentric frame¹.

The light curve has been obtained by using only detector pixels illuminated by more than 40% by the source, and binning the events with a minimum of 50 counts per time bin. The burst consisted of a main pulse of ~ 0.2 s, with two distinct peaks, and with fainter, but statistically significant emission both preceding and following it². Peak-1 coincides in time with the brightest of the peaks seen with the HXMT satellite in the 1-30 keV light curves (Zhang et al. 2020c).

The ISGRI light curve of the entire pulse can be satisfactorily fitted with the sum of 3 Gaussian curves: a broad one ($\sigma = 60$ ms) and two narrow ones

($\sigma = 2$ ms). The center of the two narrow Gaussians are at $T_1 = 14:34:24.461$ UTC and $T_2 = T_1 + 32 \pm 2$ ms. To check if this time interval corresponds to a characteristic intensity variation timescale of the source, we folded the ISGRI events at a period of 32 ms, but found no conclusive evidence of such variability, besides the two spikes apparent in Fig. 1. Any attempt to characterize the variability through power spectra or wavelet analysis gave also inconclusive results.

Intriguingly, the two radio pulses reported in Scholz & Chime/Frb Collaboration (2020) are also separated by ~ 30 ms. However, a precise alignment of the radio and X-ray light curves is not possible with the currently available public information. The red line in Fig. 1 indicates the topocentric time of 14:34:33 UTC reported by Scholz & Chime/Frb Collaboration (2020), to which we applied a time delay of 18 ms, to account for propagation to the Earth center, and a dispersion correction of 8.632 s at 400 MHz (using $DM = 332.8$ pc cm⁻³, as given in the same reference). Considering the uncertainty in the dispersion delay, it might well be possible that either peak 1 or peak 2, (or both) are in temporal coincidence with the radio pulse(s).

By examining light curves in different energy ranges we could not reveal statistically significant spectral evolution. Therefore, we extracted a time averaged spectrum from a time interval of 0.3 s starting at 14:34:24.35 UTC. The spectrum can be described by a power-law with photon index $\Gamma = 2.1 \pm 0.1$ and 20-200 keV flux of $(1.71 \pm 0.07) \times 10^{-6}$ erg s⁻¹ cm⁻² with an acceptable $\chi^2 = 18.3$ for 16 degrees of freedom³. Although a simple power-law fit is formally acceptable, we also investigated other models typically used to describe the spectra of SGR bursts, namely an exponentially cut-off power law and the sum of two blackbody functions. To estimate the uncertainties of the best fit parameters we applied the Monte Carlo Markov Chain method with Goodman-Weare algorithm (Goodman & Weare 2010) and derived the 1σ confidence intervals from the 16 and 84% percentiles of posteriors. For the cutoff power-law model we adopt Jeffreys priors for cutoff energy and normalization, and a constant prior for the photon index. We find a best-fit photon index $\Gamma = 0.75^{+0.28}_{-0.25}$, cutoff energy $E_o = 52^{+14}_{-8}$ keV and 20-200 keV flux of $(1.5 \pm 0.1) \times 10^{-6}$ erg s⁻¹ cm⁻² ($\chi^2 = 12$ for 15 d.o.f., see Fig. 2).

¹ INTEGRAL was at 128 Mm from Earth, resulting in a delay of 0.195 s for the burst to reach the Earth center. All the times quoted in this paper are corrected for the light travel time from the satellite to the Earth center, unless otherwise indicated

² This extended emission is more prominent at energies below the ISGRI range, as reported with HXMT (Zhang et al. 2020b).

³ All the spectral analysis was carried out with the Xspec software v. 12.11.0 ignoring channels below 32 keV, owing to systematic uncertainty in the response calibration. We give uncertainties at 68% confidence level in the whole paper, unless specified differently

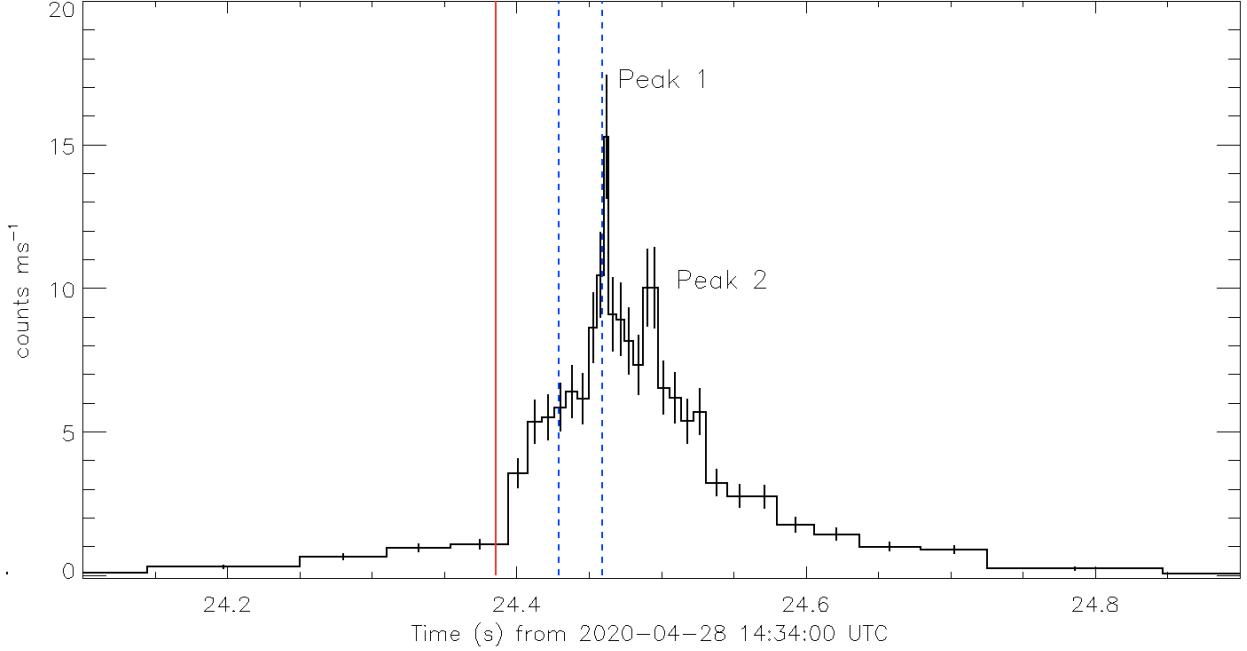


Figure 1. Light curve of burst-G in the 20-200 keV range. Peaks 1 and 2 are separated by ~ 32 ms. The red line is the time reported by [Scholz & Chime/Frb Collaboration \(2020\)](#), to which we applied a correction of 8.614 s to account for the dispersion delay at 400 MHz and conversion to the Earth center. The blue lines mark the times of the two peaks seen in the HXMT 27-250 keV light curve ([Zhang et al. 2020c,d](#)).

In the case of two black-bodies, we use Jeffreys priors for both temperatures and normalization and impose that one temperature is below 20 keV and the other one above this value. We find a best-fit with temperatures $kT_1 = 12.1 \pm 1.7$ keV, $kT_2 = 28 \pm 4$ keV and radii $R_1 = 2.0^{+0.4}_{-0.5}$ d₁₀ km, $R_2 = (0.34^{+0.15}_{-0.11})$ d₁₀ km ($\chi^2 = 11$ for 14 d.o.f.).

To measure the peak flux, we extracted a spectrum in a 0.05 s-long interval starting at 14:34:24.45 UTC. A power law gives a photon index 2.34 ± 0.16 and 20–200 keV flux of $(3.97 \pm 0.27) \times 10^{-6}$ erg s⁻¹ cm⁻² (2.3 times the average one). Fits with more complex models give poorly constrained parameters, but we checked that rescaling the overall normalization of the best fit average spectra gives acceptable and consistent descriptions.

For all the other bursts with more than 100 counts (bursts C, D, F, and I), we performed a spectral analysis with a power-law model and derived uncertainties with the Goodman Wear MCMC. The results are given in Table 2. We then computed the weighted average of their photon indexes, finding $\bar{\Gamma} = 3.2 \pm 0.5$ and imposed a Gaussian prior with these values to the photon index in the fits of the other bursts. The resulting fluences (or 3σ upper limits for bursts E and H) are also given in Table 2. We found that all the bursts detected with high signal to noise ratio have spectra softer than that

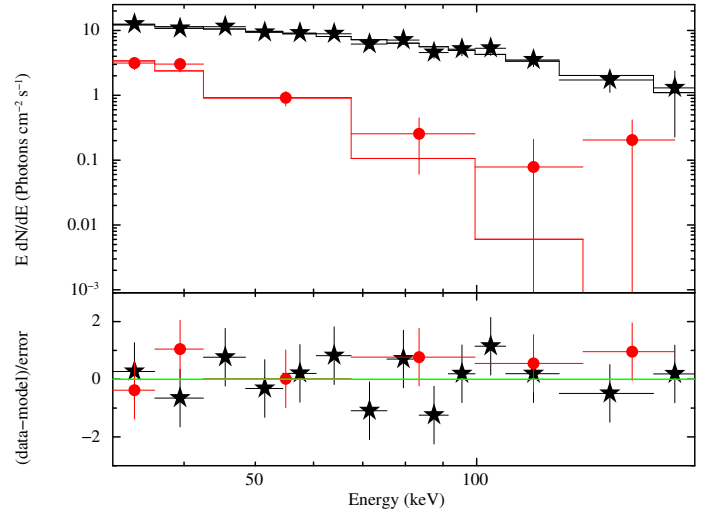


Figure 2. Unfolded spectra and fit residuals of burst-G (black stars) and burst-F (red dots) modeled using a power-law with exponential cut-off.

of burst-G. As an example, we compare in Fig. 2 the spectra of burst-G and burst-F. The latter was extracted from a 0.4 s long interval starting at 9:51:04.9 UTC and is well fit by an exponentially cut-off power law with $\Gamma = -0.3^{+0.5}_{-0.9}$, $E_o = 9 \pm 3$ keV and 20–200 keV flux of $(2.2^{+1.3}_{-0.5}) \times 10^{-7}$ erg s⁻¹ cm⁻² (χ^2 is 13 for 15 d.o.f.).

Table 2. Bursts observed in the selected observation period (see Table 1).

Name	Trigger Time YYYY-MM-DD HH:MM:SS.S	Duration s	S/N ^a	Total ^b counts	Fluence 10 ⁻⁷ erg cm ⁻²	Γ	off-axis angle(°)
A	2020-04-28 03:47:52.200	0.06	17	33 (2.1)	1.1 ^{+0.2} _{-0.3}	—	15.2
B	2020-04-28 04:09:47.300	0.09	14	35 (2.7)	0.9 ^{+0.2} _{-0.3}	—	15.2
C	2020-04-28 05:56:30.637	0.11	14	113 (10.2)	1.2 ^{+0.2} _{-0.1}	3.0 ^{+0.5} _{-0.4}	12.4
D	2020-04-28 06:07:47.037	0.17	12	110 (18.1)	0.9 ^{+0.2} _{-0.1}	3.2 ^{+0.6} _{-0.3}	12.4
E	2020-04-28 08:03:34.370	0.04	9	18 (1.8)	< 0.6	—	14.2
F	2020-04-28 09:51:04.894	0.38	10	201 (56.0)	1.0 ^{+0.4} _{-0.1}	3.8 ^{+1.2} _{-0.4}	10.4
G	2020-04-28 14:34:24.357	0.75	23	1629 (159.1)	5.9 ^{+0.2} _{-0.2}	2.1 ^{+0.1} _{-0.1}	8.1
H	2020-04-29 09:10:53.895	0.06	8	7 (0.7)	< 0.7	—	15.6
I	2020-05-03 23:25:13.469	0.15	46	136 (3.1)	9.0 ^{+1.2} _{-1.0}	3.3 ^{+0.5} _{-0.3}	16.9

^aS/N extracted from the lightcurve binned at 100 ms, which are used to detect the bursts.

^bTotal counts collected by IBIS in the time range with, between parentheses, the number of counts expected from the background.

The IBIS soft gamma-ray detector PICsIT has a spectral-timing data mode with a 7.8-ms integration time that allows the detection of impulsive events in the 200–2600 keV energy range (Ubertini et al. 2003; Labanti et al. 2003). Analysis of the spectral-timing data during burst-G yielded a 3σ upper limit of 4.5×10^{-8} erg s⁻¹ cm⁻² in the 200–500 keV energy range, assuming the cut-off power law spectral parameters from ISGRI.

Some of the bursts in Table 2 were also detected by the SPI-ACS. In particular, burst-G had a signal to noise ratio of 4.65 on a 0.65 s time scale. We note that, independently of the IBIS/ISGRI detection, the ACS data give an association with the FRB with a false alarm probability at the level of 2.9 σ .

We have also inspected JEM-X and SPI data at the time of the magnetar bursts. SPI clearly detects the brightest of the bursts listed in Table 2, but the data are affected by telemetry saturation features, complicating the analysis. The signal to noise ratio of the bursts in SPI is much lower than that in ISGRI, and we choose not to use these data in the present paper. No relevant signals were found in the JEM-X data.

A highly polarized radio flare from SGR 1935+2154 was detected by FAST on April, 30 at 21:43:00.5 UTC (Zhang et al. 2020a). At this time the source was 12.9° off-axis and we could derive a 5σ upper limit on the fluence of any burst shorter than 1 s at the level of 2.3×10^{-8} erg cm⁻² in the 20–200 keV band, assuming the spectral shape of burst-G.

4. DISTANCE ESTIMATE FROM THE DUST SCATTERING RING

A bright dust-scattering X-ray ring, with radius of $\sim 85''$, was detected around SGR 1935+2154 in a Swift/XRT observation performed on April 27, 2020

from 19:42 to 20:15 (Kennea et al. 2020). Expanding scattering rings produced by bursting sources give the possibility to derive some information on the relative distances of the emitting source and of the scattering dust by studying the time delay of scattered photons (Trümper & Schönfelder 1973). We analyzed the XRT data (obs.ID 00968211001) to derive an estimate of the SGR 1935+2154 distance.

Due to the time delay of scattered photons, the angular radius θ of a ring produced by a burst emitted at t_0 by an X-ray source at distance d_s and scattered by dust at distance D_d , increases with time t as:

$$\theta(t) = \left[\frac{827}{d_s} \frac{(1-x)}{x} (t - t_0) \right]^{1/2}, \text{ where the distances are measured in parsecs, } \theta \text{ in arcseconds, times in seconds, and } x = \frac{D_d}{d_s}.$$

The main bursting activity of SGR 1935+2154 started on April 27, 2020 at 18:26:20 (Palmer 2020), but the largest X-ray fluence was produced about 5 minutes later, in a series of bright bursts emitted within ~ 10 s (Ursi et al. 2020). We therefore assume that this "burst forest" is the origin of the X-ray ring, and fix t_0 at 18:33:10. As shown in Green et al. (2019), the interstellar dust in the direction of SGR 1935+2154 is concentrated in two nearby layers, at distances of 0.5 and 1.1 kpc, and in a farther one at ~ 6 –7 kpc. The closest dust layer is the one causing the highest optical extinction.

Using the method of Tiengo & Mereghetti (2006), we find that the rapid expansion rate of the X-ray ring is consistent with scattering from the closest dust layer. Fixing the value of D_d to 0.5 kpc, i.e. the average distance of the dust layer, we obtain for SGR 1935+2154 a distance of $d_s = 3.4^{+0.5}_{-0.4}$ kpc. This estimate does not depend much on the exact value of t_0 . If we take a

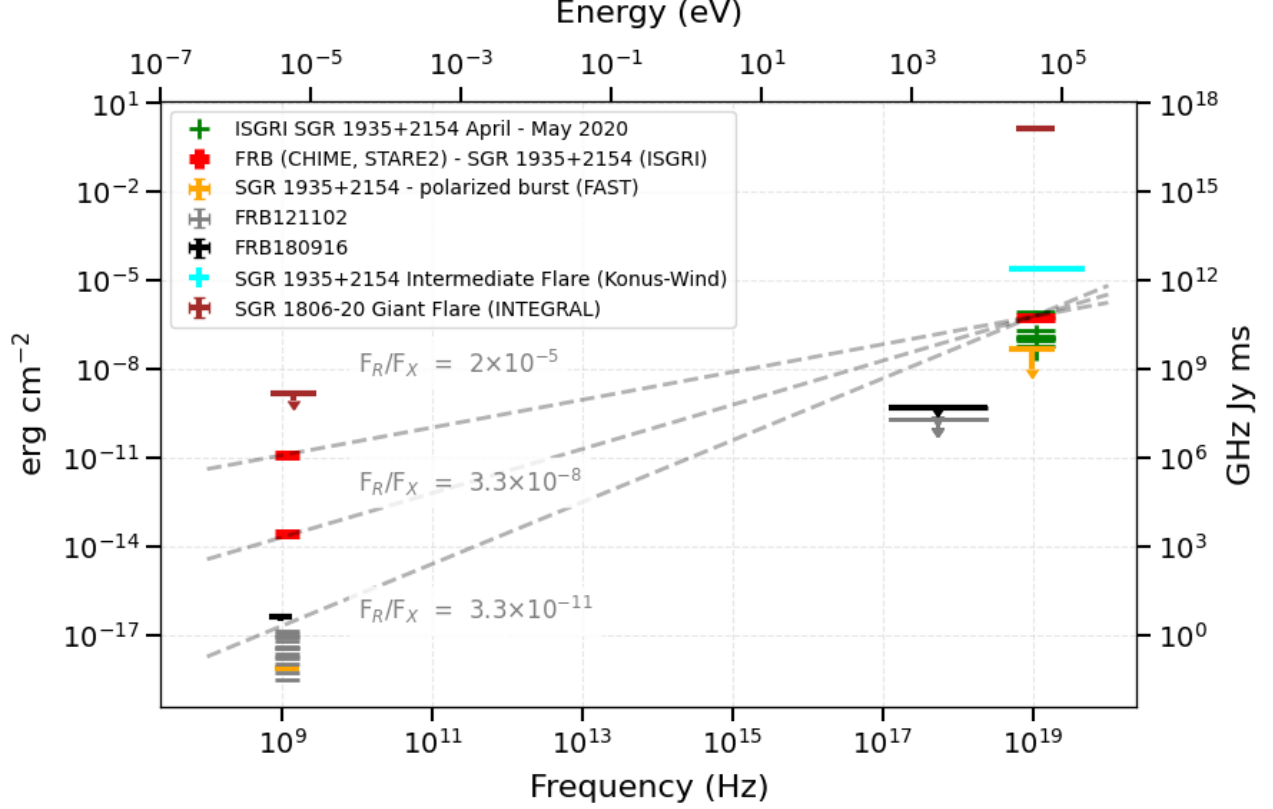


Figure 3. Comparison of the spectral energy distribution of burst-G from SGR 1935+2154 (red) with the upper limits for other magnetars and FRB obtained from simultaneous radio and X-ray observations.

more conservative approach, allowing D_d in the range 0.47-0.53 kpc, we obtain source distances in the range 2.2 – 7.1 kpc.

We note that this range of distances is consistent with an association of SGR 1935+2154 with SNR G57.2+0.8, for which a distance of 6.6 ± 0.7 kpc has been recently derived by Zhou et al. (2020).

5. DISCUSSION

Burst-G is the first burst from an SGR to be unambiguously associated with a short pulse of radio emission that, apart from a DM not exceeding the Galactic value and a much lower luminosity, shows very similar properties to extragalactic FRBs (Scholz & Chime/Frb Collaboration 2020; Bochenek et al. 2020).

Its total hard X-ray fluence, derived from the fit with a cut-off power law and corrected to account for the flux outside the spectrum integration time, is $(5.2 \pm 0.4) \times 10^{-7}$ erg cm $^{-2}$ (20-200 keV, the other models considered above give similar values). Such a fluence, and the peak flux of $\sim 4 \times 10^{-6}$ erg s $^{-1}$ cm $^{-2}$, are in the range of values previously observed for other bursts of SGR 1935+2154 (Lin et al. 2020), and, therefore, they do not qualify

burst-G as particularly energetic. They correspond to a luminosity of $\sim 5 \times 10^{40} d_{10}^2$ erg s $^{-1}$ and to a released energy of $\sim 5 \times 10^{39} d_{10}^2$ erg in the 20-200 keV range (assuming isotropic emission).

On the other hand, the spectrum of burst-G was harder than that of typical SGR bursts. Notably, it was also harder than that of the longer (~ 1.7 s) and brighter burst emitted by this source on April 12, 2015 and classified as an intermediate flare (Kozlova et al. 2016). The latter was at least a factor 10 more energetic than burst-G, but it had a smoother time profile and a softer spectrum. From the spectral point of view, the SGR 1935+2154 burst most similar to burst-G was the one detected by several satellites on April 22, 2020 (Cherry et al. 2020; Hurley et al. 2020). It had a fluence of $\sim 10^{-5}$ erg cm $^{-2}$ and a simple time profile with a single pulse lasting 0.6 s, a sharp rise time and no evidence for sub-structures (Ridnaia et al. 2020a). It is thus possible that the radio emission, detected so far only in burst-G, might be related to its particularly hard X-ray spectrum. Note that all the SGR 1935+2154 bursts in the large sample studied by Lin et al. (2020) gave, in the

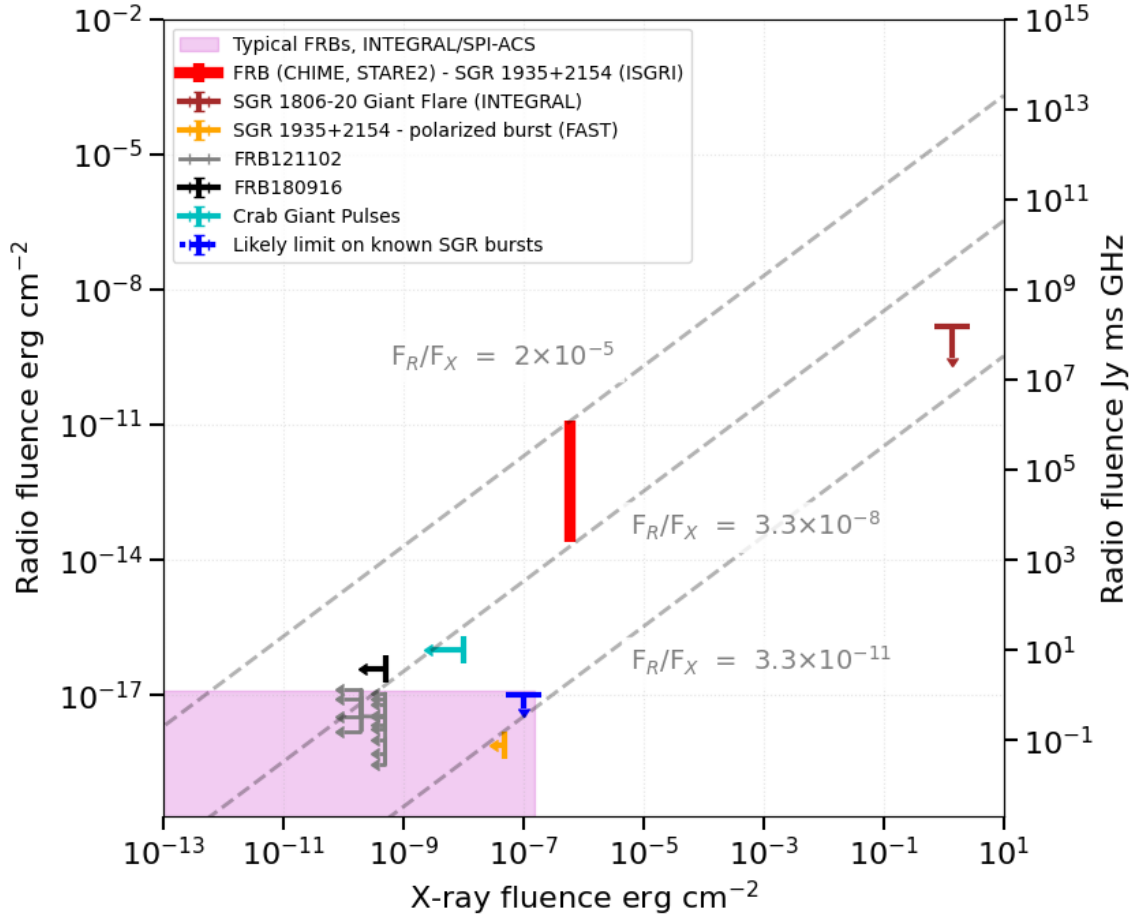


Figure 4. Radio versus X-ray (starting from 0.5 keV) fluences for FRBs and magnetar bursts. The range of FRB fluences corresponds to a variety of detections reported in the past years (see references in the text). The purple region indicates a robust upper limit on the hard X-ray fluence of FRBs as derived with high-duty-cycle detector, such as the INTEGRAL/SPI-ACS. The arrow indicating likely radio limit on known SGR bursts assumes that monitoring of FRB searches (for example CHIME) produced upper limits corresponding to typical sensitivity to FRBs at the time of known SGR 1935+2154 burst.

two blackbody fits, average temperatures a factor ~ 2 smaller than those of burst-G.

The double peaked time profile of burst-G seen in the ISGRI light curve is particularly interesting because the 400-800 MHz emission seen with CHIME consisted of two pulses separated by about 30 ms (Scholz & Chime/Frb Collaboration 2020). We note that also the light curves measured with other instruments (Konus-Wind, Ridnaia et al. 2020b; HXMT, Zhang et al. 2020c), show a time profile comprising a few narrow peaks with separations similar to that between the two radio pulses.

Explanations involving magnetars at extragalactic or cosmological distances have been among the first ones to be proposed for FRB (Popov & Postnov 2007). Several models have been developed, based on scenarios for which high-energy emission can be expected in the form of prompt bursts (e.g. Lyubarsky (2014); Beloborodov (2017, 2019); Lyubarsky (2020)) or as a long lasting af-

terglow following the FRB (Murase et al. 2017). However, all the searches for X/ γ -ray counterparts of FRB carried out up to now have been unsuccessful⁴ (Scholz et al. 2017; Xi et al. 2017; Martone et al. 2019; Guidorzi et al. 2019; Cunningham et al. 2019; Anumalapudi et al. 2020).

Tendulkar et al. (2016) derived lower limits on the ratio between radio (1.4 GHz) and X/ γ -ray (>30 keV) fluences $\eta_{FRB} > 10^{7-9}$ Jy ms $\text{erg}^{-1} \text{cm}^2$ for 15 FRBs. Negative results were found also with coordinated multiwavelength observations of FRB 180916.J0158+65 (Scholz et al. 2020; Pilia et al. 2020; Tavani et al. 2020),

⁴ The claimed association of a ~ 400 s long X-ray transient with FRB 131104 (DeLaunay et al. 2016) has not been supported by subsequent observations (Shannon & Ravi 2017). In any case, the properties of this transient are very different from those of burst-G.

that has been considered as a promising target, owing to its close distance of 150 Mpc and periodic behavior of the radio burst emission. Similarly, searches for FRB associated with magnetar bursts provided only upper limits (Burgay et al. 2018), including the case of the December 2004 giant flare from SGR 1806–20, for which Tendulkar et al. (2016) derived $\eta_{FRB} < 10^7$ Jy ms erg $^{-1}$ cm 2 .

Despite the large uncertainty in the preliminary radio measurements reported for burst-G (a few kJy ms at 400–800 MHz (Scholz & Chime/Frb Collaboration 2020), a few MJy at 1.4 GHz Bochenek et al. (2020)), it is interesting to compare the spectral energy distribution of SGR 1935+2154 (Fig. 3) and the ratio of its radio and X-ray fluences F_R/F_X (Fig. 4) with the limits obtained for similar sources.

Burst-G was characterized by a very large value of F_R/F_X in the range $\sim 3 \times 10^{-8} - 10^{-5}$. This high ratio is consistent with the lack of detection of high-energy emission in extragalactic FRB, as it can be seen by scaling the fluences to distances of a few hundreds of Mpc (i.e. a factor of order 10^{8-9}). On the other hand, such a high F_R/F_X is at variance with the limit derived for the SGR 1806–20 giant flare. This might suggest that giant flares and ordinary SGR bursts are indeed different phenomena, as it is also supported by their different spectral and timing properties, and/or that magnetar bursts can have a large range of F_R/F_X . It must also be considered that both the radio and high-energy emissions could be non-isotropic and beamed in different directions, thus complicating the observational picture and making it difficult to draw strong conclusions until a much larger sample of bursts is observed.

The possible precise time coincidence between the radio pulses and the narrow peaks of burst-G, if confirmed, places constraints on the emission region. Unless particularly *ad hoc* geometries are invoked, a time coincidence within Δt implies that the radio and high-energy photons are emitted at the same time and in regions separated by less than $3 \times 10^8 (\Delta t/10 \text{ ms})$ cm. Considering that SGR 1935+2154 has a light cylinder radius $Pc/2\pi = 1.5 \times 10^{10}$ cm, even a coincidence within $\Delta t \sim 0.1$ s would be fully consistent with models that place the emission region within the neutron star magnetosphere (e.g. (Lyutikov 2002; Lyubarsky 2020)).

6. CONCLUSIONS

The discovery of simultaneous fast bursting emission at radio and high-energy from the galactic SGR 1935+2154 supports models based on magnetars for extragalactic FRBs, although the latter involve a

much larger energy output compared to the case discussed here.

If all extragalactic FRBs are characterized by ratios of radio to X-ray fluences as large as that of burst-G (using the \sim MJy flux reported in Bochenek et al. (2020)), their detection with current high-energy satellites will be difficult. However, since it is clear that a single fluence ratio is not compatible with all available measurements (see Fig. 4), only future multi-wavelength (and especially high-duty-cycle hard X-ray) observations of FRBs will reveal how unusual was the, so far single, joint detection obtained for SGR 1935+2154.

We expect that many more radio bursts will be soon detected from Galactic magnetars. These observation will establish if, as it is suggested by the INTEGRAL data, radio emission is associated only to the spectrally hardest SGR bursts or it is a more common property.

Finally, a comment on the role of magnetars in the context of both Gamma-ray bursts (GRBs) and FRBs. In the first years following their discovery, GRBs and SGRs were believed to belong to the same phenomenological class of short-lived high-energy transients of mysterious origin. However, SGRs distinguishing features of repetitive behaviour, giant flares, pulsations and association with supernova remnants along the galactic plane, convincingly demonstrated they belonged to a different population, that of galactic magnetars. On the other hand, GRBs were confirmed as cosmological sources, putting to rest one of the biggest controversies in astrophysics of the previous few decades. Newly born magnetars can also be considered as possible central engines for powering extragalactic GRBs, while a small fraction of the short-duration GRBs may be due to extragalactic magnetar giant flares.

Mirroring this GRB-SGR-magnetar entanglement, the observation of FRB-like radio emission and gamma-ray flares from the known galactic magnetar SGR 1935+2154 now opens the possibility that a subset of the currently known population of FRBs consists of galactic magnetars so far unidentified at other wavelengths, while also providing strong support for a magnetar origin of the extragalactic FRBs.

ACKNOWLEDGMENTS

Based on observations with INTEGRAL, an ESA project with instruments and science data centre funded by ESA member states (especially the PI countries: Denmark, France, Germany, Italy, Switzerland, Spain) and with the participation of Russia and the USA. IS-GRI has been realized and maintained in-flight by CEA-Saclay/Irfu with the support of CNES. The Italian authors acknowledge support via ASI/INAF Agreement n. 2019-35-HH and PRIN-MIUR 2017 UnIAM (Unifying Isolated and Accreting Magnetars, PI S.Mereghetti). D.G. acknowledges the financial support of the UnivEarthS LabEx (ANR-10-LABX-0023 and ANR-18-IDEX-0001).

REFERENCES

- Anumalapudi, A., Bhalariao, V., Tendulkar, S. P., & Balasubramanian, A. 2020, *ApJ*, 888, 40, doi: [10.3847/1538-4357/ab5363](https://doi.org/10.3847/1538-4357/ab5363)
- Beloborodov, A. M. 2017, *ApJL*, 843, L26, doi: [10.3847/2041-8213/aa78f3](https://doi.org/10.3847/2041-8213/aa78f3)
- . 2019, arXiv e-prints, arXiv:1908.07743, <https://arxiv.org/abs/1908.07743>
- Bochenek, C., Kulkarni, S., Ravi, V., et al. 2020, *The Astronomer’s Telegram*, 13684, 1
- Burgay, M., Esposito, P., Israel, G. L., et al. 2018, in *IAU Symposium*, Vol. 337, *Pulsar Astrophysics the Next Fifty Years*, ed. P. Weltevrede, B. B. P. Perera, L. L. Preston, & S. Sanidas, 319–321, doi: [10.1017/S1743921317008547](https://doi.org/10.1017/S1743921317008547)
- Burgay, M., Israel, G. L., Rea, N., et al. 2014, *The Astronomer’s Telegram*, 6371, 1
- Cherry, M. L., Yoshida, A., Sakamoto, T., et al. 2020, *GRB Coordinates Network*, 27623, 1
- Cordes, J. M., & Chatterjee, S. 2019, *ARA&A*, 57, 417, doi: [10.1146/annurev-astro-091918-104501](https://doi.org/10.1146/annurev-astro-091918-104501)
- Courvoisier, T. J. L., Walter, R., Beckmann, V., et al. 2003, *A&A*, 411, L53, doi: [10.1051/0004-6361:20031172](https://doi.org/10.1051/0004-6361:20031172)
- Cunningham, V., Cenko, S. B., Burns, E., et al. 2019, *ApJ*, 879, 40, doi: [10.3847/1538-4357/ab2235](https://doi.org/10.3847/1538-4357/ab2235)
- DeLaunay, J. J., Fox, D. B., Murase, K., et al. 2016, *ApJL*, 832, L1, doi: [10.3847/2041-8205/832/1/L1](https://doi.org/10.3847/2041-8205/832/1/L1)
- Fletcher, C., & Fermi GBM Team. 2020, *GRB Coordinates Network*, 27659, 1
- Goldwurm, A., David, P., Foschini, L., et al. 2003, *A&A*, 411, L223, doi: [10.1051/0004-6361:20031395](https://doi.org/10.1051/0004-6361:20031395)
- Goodman, J., & Weare, J. 2010, *Communications in Applied Mathematics and Computational Science*, 5, 65, doi: [10.2140/camcos.2010.5.65](https://doi.org/10.2140/camcos.2010.5.65)
- Green, G. M., Schlafly, E., Zucker, C., Speagle, J. S., & Finkbeiner, D. 2019, *ApJ*, 887, 93, doi: [10.3847/1538-4357/ab5362](https://doi.org/10.3847/1538-4357/ab5362)
- Guidorzi, C., Marongiu, M., Martone, R., et al. 2019, *ApJ*, 882, 100, doi: [10.3847/1538-4357/ab3408](https://doi.org/10.3847/1538-4357/ab3408)
- Hurley, K., Mitrofanov, I. G., Golovin, D., et al. 2020, *GRB Coordinates Network*, 27625, 1
- Israel, G. L., Esposito, P., Rea, N., et al. 2016, *MNRAS*, 457, 3448, doi: [10.1093/mnras/stw008](https://doi.org/10.1093/mnras/stw008)
- Kaspi, V. M., & Beloborodov, A. M. 2017, *ARA&A*, 55, 261, doi: [10.1146/annurev-astro-081915-023329](https://doi.org/10.1146/annurev-astro-081915-023329)
- Kennea, J. A., Beardmore, A. P., Page, K. L., & Palmer, D. M. 2020, *The Astronomer’s Telegram*, 13679, 1
- Kothes, R., Sun, X., Gaensler, B., & Reich, W. 2018, *ApJ*, 852, 54, doi: [10.3847/1538-4357/aa9e89](https://doi.org/10.3847/1538-4357/aa9e89)
- Kozlova, A. V., Israel, G. L., Svinkin, D. S., et al. 2016, *MNRAS*, 460, 2008, doi: [10.1093/mnras/stw1109](https://doi.org/10.1093/mnras/stw1109)
- Labanti, C., Di Cocco, G., Ferro, G., et al. 2003, *A&A*, 411, L149, doi: [10.1051/0004-6361:20031356](https://doi.org/10.1051/0004-6361:20031356)
- Lebrun, F., Leray, J. P., Lavocat, P., et al. 2003, *A&A*, 411, L141, doi: [10.1051/0004-6361:20031367](https://doi.org/10.1051/0004-6361:20031367)
- Levan, A., Kouveliotou, C., & Fruchter, A. 2018, *ApJ*, 854, 161, doi: [10.3847/1538-4357/aaa88d](https://doi.org/10.3847/1538-4357/aaa88d)
- Lin, L., Gogus, E., Roberts, O. J., et al. 2020, arXiv e-prints, arXiv:2003.10582, <https://arxiv.org/abs/2003.10582>
- Lyubarsky, Y. 2014, *MNRAS*, 442, L9, doi: [10.1093/mnrasl/slu046](https://doi.org/10.1093/mnrasl/slu046)
- . 2020, arXiv e-prints, arXiv:2001.02007, <https://arxiv.org/abs/2001.02007>
- Lyutikov, M. 2002, *ApJL*, 580, L65, doi: [10.1086/345493](https://doi.org/10.1086/345493)

- Marcote, B., Nimmo, K., Hessels, J. W. T., et al. 2020, *Nature*, 577, 190, doi: [10.1038/s41586-019-1866-z](https://doi.org/10.1038/s41586-019-1866-z)
- Martone, R., Guidorzi, C., Margutti, R., et al. 2019, *A&A*, 631, A62, doi: [10.1051/0004-6361/201936284](https://doi.org/10.1051/0004-6361/201936284)
- Mereghetti, S., Götz, D., Borkowski, J., Walter, R., & Pedersen, H. 2003, *A&A*, 411, L291, doi: [10.1051/0004-6361:20031289](https://doi.org/10.1051/0004-6361:20031289)
- Mereghetti, S., Pons, J. A., & Melatos, A. 2015, *SSRv*, 191, 315, doi: [10.1007/s11214-015-0146-y](https://doi.org/10.1007/s11214-015-0146-y)
- Murase, K., Mészáros, P., & Fox, D. B. 2017, *ApJL*, 836, L6, doi: [10.3847/2041-8213/836/1/L6](https://doi.org/10.3847/2041-8213/836/1/L6)
- Olausen, S. A., & Kaspi, V. M. 2014, *ApJS*, 212, 6, doi: [10.1088/0067-0049/212/1/6](https://doi.org/10.1088/0067-0049/212/1/6)
- Palmer, D. M. 2020, *The Astronomer's Telegram*, 13675, 1
- Palmer, D. M., Barthelmy, S., Gehrels, N., et al. 2005, *Nature*, 434, 1107, doi: [10.1038/nature03525](https://doi.org/10.1038/nature03525)
- Pearlman, A. B., Majid, W. A., Prince, T. A., Naudet, C. J., & Kocz, J. 2020, *The Astronomer's Telegram*, 13713, 1
- Petroff, E., Hessels, J. W. T., & Lorimer, D. R. 2019, *A&A Rv*, 27, 4, doi: [10.1007/s00159-019-0116-6](https://doi.org/10.1007/s00159-019-0116-6)
- Pilia, M., Burgay, M., Possenti, A., et al. 2020, arXiv e-prints, arXiv:2003.12748. <https://arxiv.org/abs/2003.12748>
- Platts, E., Weltman, A., Walters, A., et al. 2019, *PhR*, 821, 1, doi: [10.1016/j.physrep.2019.06.003](https://doi.org/10.1016/j.physrep.2019.06.003)
- Popov, S. B., & Postnov, K. A. 2007, arXiv e-prints, arXiv:0710.2006. <https://arxiv.org/abs/0710.2006>
- Ranasinghe, S., Leahy, D. A., & Tian, W. 2018, *Open Physics Journal*, 4, 1, doi: [10.2174/1874843001804010001](https://doi.org/10.2174/1874843001804010001)
- Ravi, V., Catha, M., D'Addario, L., et al. 2019, *Nature*, 572, 352, doi: [10.1038/s41586-019-1389-7](https://doi.org/10.1038/s41586-019-1389-7)
- Ridnaia, A., Golenetskii, S., Aptekar, R., et al. 2020a, *GRB Coordinates Network*, 27631, 1
- . 2020b, *The Astronomer's Telegram*, 13688, 1
- Scholz, P., & Chime/Frb Collaboration. 2020, *The Astronomer's Telegram*, 13681, 1
- Scholz, P., Bogdanov, S., Hessels, J. W. T., et al. 2017, *ApJ*, 846, 80, doi: [10.3847/1538-4357/aa8456](https://doi.org/10.3847/1538-4357/aa8456)
- Scholz, P., Cook, A., Cruces, M., et al. 2020, arXiv e-prints, arXiv:2004.06082. <https://arxiv.org/abs/2004.06082>
- Shannon, R. M., & Ravi, V. 2017, *ApJL*, 837, L22, doi: [10.3847/2041-8213/aa62fb](https://doi.org/10.3847/2041-8213/aa62fb)
- Stamatikos, M., Malesani, D., Page, K. L., & Sakamoto, T. 2014, *GRB Coordinates Network*, 16520, 1
- Surnis, M. P., Krishnakumar, M. A., Maan, Y., Joshi, B. C., & Manoharan, P. K. 2014, *The Astronomer's Telegram*, 6376, 1
- Tavani, M., Verrecchia, F., Casentini, C., et al. 2020, *ApJL*, 893, L42, doi: [10.3847/2041-8213/ab86b1](https://doi.org/10.3847/2041-8213/ab86b1)
- Tendulkar, S. P., Kaspi, V. M., & Patel, C. 2016, *ApJ*, 827, 59, doi: [10.3847/0004-637X/827/1/59](https://doi.org/10.3847/0004-637X/827/1/59)
- Tiengo, A., & Mereghetti, S. 2006, *A&A*, 449, 203, doi: [10.1051/0004-6361:20054162](https://doi.org/10.1051/0004-6361:20054162)
- Trümper, J., & Schönfelder, V. 1973, *A&A*, 25, 445
- Turolla, R., Zane, S., & Watts, A. L. 2015, *Reports on Progress in Physics*, 78, 116901, doi: [10.1088/0034-4885/78/11/116901](https://doi.org/10.1088/0034-4885/78/11/116901)
- Ubertini, P., Lebrun, F., Di Cocco, G., et al. 2003, *A&A*, 411, L131, doi: [10.1051/0004-6361:20031224](https://doi.org/10.1051/0004-6361:20031224)
- Ursi, A., Pittori, C., Tempesta, P., et al. 2020, *The Astronomer's Telegram*, 13682, 1
- Veres, P., Bissaldi, E., Briggs, M. S., & Fermi GBM Team. 2020, *GRB Coordinates Network*, 27531, 1
- Xi, S.-Q., Tam, P.-H. T., Peng, F.-K., & Wang, X.-Y. 2017, *ApJL*, 842, L8, doi: [10.3847/2041-8213/aa74cf](https://doi.org/10.3847/2041-8213/aa74cf)
- Younes, G., Kouveliotou, C., Jaodand, A., et al. 2017, *ApJ*, 847, 85, doi: [10.3847/1538-4357/aa899a](https://doi.org/10.3847/1538-4357/aa899a)
- Younes, G., Guver, T., Enoto, T., et al. 2020, *The Astronomer's Telegram*, 13678, 1
- Zhang, C. F., Jiang, J. C., Men, Y. P., et al. 2020a, *The Astronomer's Telegram*, 13699, 1
- Zhang, S. N., Zhang, B., & Lu, W. B. 2020b, *The Astronomer's Telegram*, 13692, 1
- Zhang, S. N., Xiong, S. L., Li, C. K., et al. 2020c, *The Astronomer's Telegram*, 13696, 1
- Zhang, S. N., Li, C. K., Zheng, S. J., et al. 2020d, *The Astronomer's Telegram*, 13704, 1
- Zhou, P., Zhou, X., Chen, Y., et al. 2020, arXiv e-prints, arXiv:2005.03517. <https://arxiv.org/abs/2005.03517>